Combustion and Flame 158 (2011) 1032–1036

Contents lists available at ScienceDirect

Combustion and Flame

journal homepage: www.elsevier.com/locate/combustflame

Detailed chemical kinetic mechanisms of ethyl methyl, methyl *tert*-butyl and ethyl *tert*-butyl ethers: The importance of uni-molecular elimination reactions

K. Yasunaga [a], J.M. Simmie [a], H.J. Curran [a,*], T. Koike [b], O. Takahashi [c], Y. Kuraguchi [d], Y. Hidaka [d]

[a] Combustion Chemistry Centre, NUI Galway, Ireland
[b] Department of Applied Chemistry, National Defense Academy, Yokosuka, Japan
[c] Department of Chemistry, Graduate of Science, Hiroshima University, Higashihiroshima, Japan
[d] Chemistry and Biology, Graduate School of Science and Engineering, Ehime University, Matsuyama, Japan

ARTICLE INFO

Article history:
Received 11 August 2010
Received in revised form 21 September 2010
Accepted 19 October 2010
Available online 17 November 2010

Keywords:
Shock tube
Unimolecular reaction
Detailed reaction mechanism

ABSTRACT

A reaction mechanism of ethyl methyl ether (EME), methyl *tert*-butyl ether (MTBE) and ethyl *tert*-butyl ether (ETBE) for pyrolysis and oxidation have been constructed using the same method applied to di-ethyl ether (DEE) in our recent work [1]. The mechanism, comprising of 1051 reactions involving 215 species, was tested against the experimental data obtained using shock tubes with good agreement. It was found that the uni-molecular elimination reaction has a larger influence on the pyrolysis and oxidation of MTBE and ETBE compared to EME and DEE at high temperatures. The energy barrier height between reactants and transition states of molecular elimination reactions calculated by high level *ab initio* MO methods has revealed the difference in reactivity among the four ethers. It is also shown that ETBE or MTBE inhibit the reactivity of an equi-molar 2% mixture of hydrogen and oxygen, whereas EME and DEE do not inhibit reactivity.

1. Objective

To reduce the use of fossil fuels, ethers (structures of these are shown in Fig. 1) have attracted considerable attention as one of the most suitable alternative fuels. For example, the characteristics of the combustion of ETBE [2,3] have been investigated. Very recently we successfully constructed a chemical kinetic model to describe the oxidation of di-ethyl ether [1] at high temperatures. The chemical kinetic model of DEE includes a uni-molecular elimination reaction to form ethanol and ethylene, and simple C—C and C—O bond fission and hydrogen atom abstraction by radicals such as $\dot{H}$, $\dot{O}H$ and $\dot{C}H_3$. EME, MTBE and ETBE also include similar reactions. In this study, we apply the same method used to construct our DEE mechanism to the other ethers, and examine if it is universally applicable to all ethers. We also discuss the difference in reactivity that has been shown [1,4–6] among ethers.

2. Experimental

Samples of EME, DEE, MTBE and ETBE fuels (99.0% pure) were supplied by Wako Pure Chemical, and de-gassed through a series of freeze–pump–thaw cycles, after which no more gas was observed to escape on thawing the solid. Argon (99.9999% pure) was supplied by Iwatani. Mixtures were prepared using the method of partial pressures. The incident shock velocity at the end wall was used to calculate the temperature and pressures of the mixture behind the reflected shock wave using the equilibrium program Gaseq [7].

Two shock tubes, of which surfaces of the inner reaction sections are un-polished, were used in this study. The first with 4.1 cm i.d. was a magic-hole-type (magic-hole-type shock tube: MHST). A simple description is only given below, as the apparatus has previously been described in detail by Hidaka et al. [8–11]. The reacted gas mixtures, quenched using the single pulse method, were extracted into a pre-evacuated vessel (50 cm^3) through a valve near the end-plate. These mixtures were then analyzed using three serially connected gas chromatographs (GCs), each having a thermal conductivity detector (TCD) [10,11]. GC analyses were carried out using a Shimadzu GC-8A with a 2 m column packed with Sebaconitrile and heated to 75 °C to determine the concentrations of EME, DEE, MTBE, ETBE, C_2H_5OH, CH_3CHO, CH_3OH and hydrocarbons above C_4. A Shimadzu GC-8A2 with a 2 m column packed with Porapak Q connected to a 2 m column packed with Unibeads 1S was used to determine the concentrations of C_2H_6, C_2H_4, C_2H_2, C_3H_8, C_3H_6, C_3H_4-a (allene), C_3H_4-p (propyne) and CO_2, and these columns were heated at a rate of 3 °C/min from 50 °C to 130 °C. A Shimadzu GC-3BT with a 2 m column packed with Molecular Sieve 5A at 50 °C was used to determine the concentrations of

* Corresponding authors. Tel.: +353 91 493856; fax: +353 91 525700 (K. Yasunaga), tel.: +353 91 494082 (H.J. Curran).
E-mail addresses: kenji.yasunaga@nuigalway.ie, yasunaga@nda.ac.jp (K. Yasunaga), henry.curran@nuigalway.ie (H.J. Curran).
URL: http://c3.nuigalway.ie/ (H.J. Curran).

0010-2180/$ - see front matter © 2010 The Combustion Institute. Published by Elsevier Inc. All rights reserved.
doi:10.1016/j.combustflame.2010.10.012

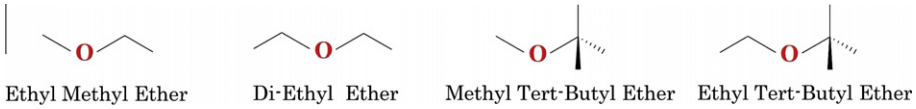

Fig. 1. Structures of ethyl methyl ether (EME), di-ethyl ether (DEE), methyl *tert*-butyl ether (MTBE) and ethyl *tert*-butyl ether (ETBE).

CH_4 and CO. Helium was used as the carrier gas. The output signal from each GC was introduced into Shimadzu Chromatopac C-R3A1, C-R3A2, and C-R1B data processors. An effective heating time, t_e, (reaction time), defined as the time between the arrival of the reflected shock wave and the point at which the reflected shock pressure had fallen by 20%, was determined with an accuracy of ±5% using a method described previously [9,10]. Assuming the adiabatic expansion of a non-reactive mixture, the temperature drops by 8.5% from its initial value at the effective heating time.

Given that single pulse shock tubes have cooling rates of 6.6×10^5 K s^{-1} [8], it can be assumed that the reaction was frozen at the effective heating time, the concentrations of carbon-containing compounds and hydrogen, determined by gas chromatography, were compared with those from the simulation. The validity of effective heating time and cooling rate was tested for N_2O pyrolysis previously [8]. The experimental uncertainties of the concentrations are less than 2% except C_2H_5OH and CH_3OH due to strong adsorption. The estimated experimental uncertainty of the concentration of C_2H_5OH and CH_3OH were less than ±30%.

The second shock tube with 4.1 cm i.d. was a standard-type (standard-type shock tube: STST) connected to UV absorption equipment [12]. A light at 306.7 nm from a microwave discharge of H_2O in He through a 4.1 cm path-length in the shock tube, dispersed by a grating monochromator, was monitored with a photomultiplier, using the same method as described previously [8,11,12]. The extinction coefficient of the $\dot{O}H$ radical at 306.7 nm used in the simulation is $10^{-3.51} \times T^{+7.3}$ cm^2 mol^{-1}, which was estimated from the partial equilibrium of $\dot{O}H$ radical in the 1.0% H_2, 1.0% O_2 mixture diluted with Ar.

3. Model

The same method used to construct a chemical kinetic model to describe the oxidation of DEE [1] was applied to EME, MTBE and ETBE. The details are described below. The thermodynamic data for ethers were calculated using the THERM program of Ritter and Bozzelli [13], based on the group additivity methods developed by Benson [14]. Some data could be checked against NIST WebBook [15] and the estimated values shows good agreement. The thermodynamic data for ethers are provided in the Supplementary Material 1. The high-pressure limit rate constants for simple fission reactions were calculated based on microscopic reversibility using an estimate of the rate constant in the reverse direction for radical–radical recombination. For the recombination reactions of methoxy, ethoxy and *tert*-buthoxy radicals with alkyl radical to form EME, MTBE and ETBE a rate constant of 3.0×10^{13} mol^{-1} s^{-1} was used similar to that for methoxy radical recombination with methyl radical [16]. EME, MTBE and ETBE have C—C bond fission reactions as described below:

$$EME(+M) = CH_3O\dot{C}H_2 + \dot{C}H_3(+M) \quad (754)$$

$$MTBE(+M) = i\dot{C}_3H_6OCH_3 + \dot{C}H_3(+M) \quad (782)$$

$$ETBE(+M) = i\dot{C}_3H_6OC_2H_5 + \dot{C}H_3(+M) \quad (803)$$

$$ETBE(+M) = tC_4H_9O\dot{C}H_2 + \dot{C}H_3(+M) \quad (802)$$

A rate constant of $1.93 \times 10^{14}T^{-0.31}$ cm^3 mol^{-1} s^{-1} was used for reactions (–754) and (–802) as recommended by Tsang [17] for the recombination of methyl and *n*-propyl radicals to form *n*-butane. For reaction (–782) and (–803) a rate constant of 1.63×10^{13} exp(300/T) cm^3 mol^{-1} s^{-1} was used as recommended by Tsang [18] for recombination of methyl and *tert*-butyl radicals to form *neo*-pentane. Ethers also include complex fission reactions, so called, molecular elimination reactions. The high-pressure limit rate constants for molecular elimination reactions (804) and (805) were estimated in our previous work [6].

$$ETBE = iC_4H_8 + C_2H_5OH \quad (804)$$

$$ETBE = C_2H_4 + tC_4H_9OH \quad (805)$$

The high-pressure limit rate constants for reactions (783) and (755) are estimated by analogy with the uni-molecular elimination reaction of ethyl *tert*-butyl ether (ETBE).

$$MTBE = iC_4H_8 + CH_3OH \quad (783)$$

$$EME = C_2H_4 + CH_3OH \quad (755)$$

The values of the frequency factor proposed by Yasunaga et al. for reaction (804) and (805) were adopted for reactions (783) and (755). The barrier height energies between reactants and transition states for reactions (783) and (755) of 60.8 and 65.2 kcal mol^{-1} were used as activation energies, which were calculated using the Gaussian 03 application [19] at the MP4/cc-pVTZ//MP2/cc-pVTZ level of theory with zero point corrections. Cartesian coordinates and vibrational frequencies for all ethers and transition states, and barrier heights between products and transition states are provided in the Supplementary Material 2. A chemical activation formulation based on Quantum Rice–Ramsperger–Kassel (QRRK) theory, as described by Dean [20,21] was then used together with the high-pressure limit expressions to develop pressure-dependent rate constants which were fit to a nine-parameter Troe formalism [22].

Rate constants for hydrogen abstraction by $\dot{H}$, $\dot{C}H_3$ and $\dot{O}H$ radicals from the α and β positions were considered in this study. The rate constants for hydrogen abstraction by $\dot{H}$ and $\dot{O}H$ radicals from the α position were taken from the work of Ogura et al. [23] and Zhou et al. [24], while those for abstraction by $\dot{C}H_3$ radicals are taken from Orme et al. [25] by analogy with hydrogen atom abstraction from an alkane. Those for abstraction by $\dot{H}$ atom, $\dot{O}H$ and $\dot{C}H_3$ radicals from the β position were taken to be analogous to primary hydrogen atom abstraction from an alkane and were also taken from the work of Orme et al. [25]. The sub-mechanism of C0–C4 hydrocarbon chemistry is the same as the recent natural gas [26–31], *n*-butane [32] and *iso*-butane [33] mechanisms and their blends [34], published from this laboratory.

4. Comparison to experiment

Simulations were performed using Chemkin-Pro [35], employing the Closed Homogeneous Batch Reactor model at constant volume for shock tube experiments.

The species profiles measured in the magic-hole-type shock tube (MHST) have already been published previously [1,4–6]. Major species profiles were simulated for mixtures of 2% EME, 2% DEE, 1% MTBE and 3% ETBE diluted with argon in the pressure range 1.0–3.5 atm. The results are shown in Figs. 2–5. The simulated results show good agreement with experimental results for all ether fuels. Here we focus on the uni-molecular elimination reactions to

form alcohols and alkenes. EME, DEE, MTBE and ETBE produce methanol or ethanol or *tert*-butyl alcohol via reactions (670), (755), (783), (804) and (805).

$$DEE = C_2H_4 + C_2H_5OH \quad (670)$$

$$EME = C_2H_4 + CH_3OH \quad (755)$$

$$MTBE = iC_4H_8 + CH_3OH \quad (783)$$

$$ETBE = iC_4H_8 + C_2H_5OH \quad (804)$$

$$ETBE = C_2H_4 + tC_4H_9OH \quad (805)$$

The simulated concentrations of alcohol produced at 1300 K are 5.1% of *tert*-butyl alcohol from ETBE via (804), 8.63% of ethanol from DEE via (670), 10.8% of methanol from EME via (755), 55.9% of ethanol from ETBE via (805), 62.1% of methanol from MTBE via (783), respectively. The concentrations of ethanol from ETBE, and methanol from MTBE are much higher than the other cases by factors of 7–10. The value of the frequency factor applied to MTBE and ETBE to form iso-butene and methanol, and iso-butene and ethanol is 1.7×10^{14} s^{-1}, which corresponds to 5.7×10^{13} s^{-1} per methyl group in the *tert*-butyl group. The value of the frequency factor applied to the other methyl groups in EME, DEE and ETBE was 5.0×10^{13} s^{-1} per methyl group. These two values are only 14% different so the variation in rate constants stems from the activation energy differences. The

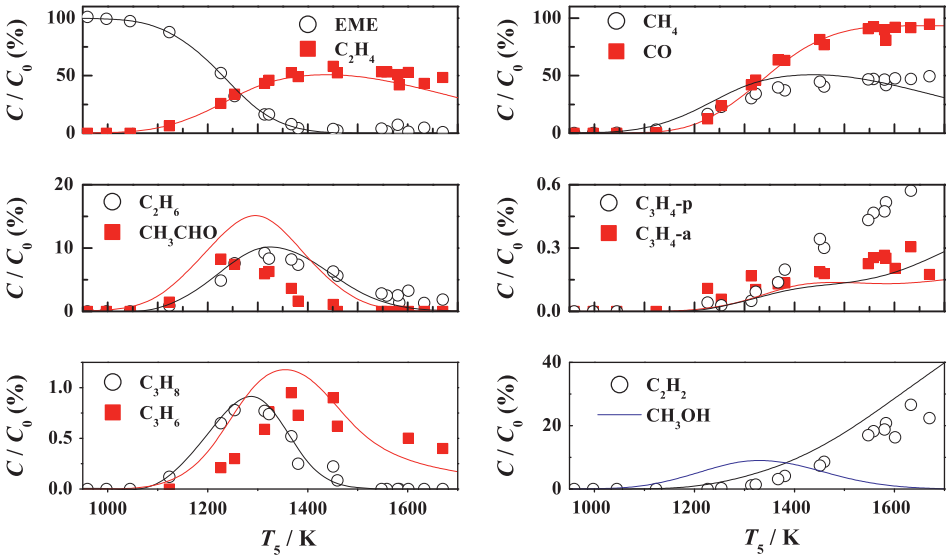

Fig. 2. Species profiles from the MHST for 2.0% EME diluted in Ar at 1.0–3.0 atm, lines simulation and symbols experiment. C_0 and C denote initial concentration of EME and concentration of chemical species after shock heat. Effective heating times used at 900 K, 1000 K, 1100 K, 1200 K, 1300 K, 1400 K, 1500 K, 1600 K and 1700 K were 3090, 2920, 2740, 2570, 2390, 2210, 2040, 1860 and 1690 μs, respectively. The concentration of CH_3OH was not measured due to the strong adsorption of CH_3OH. Only simulation result for CH_3OH is given here.

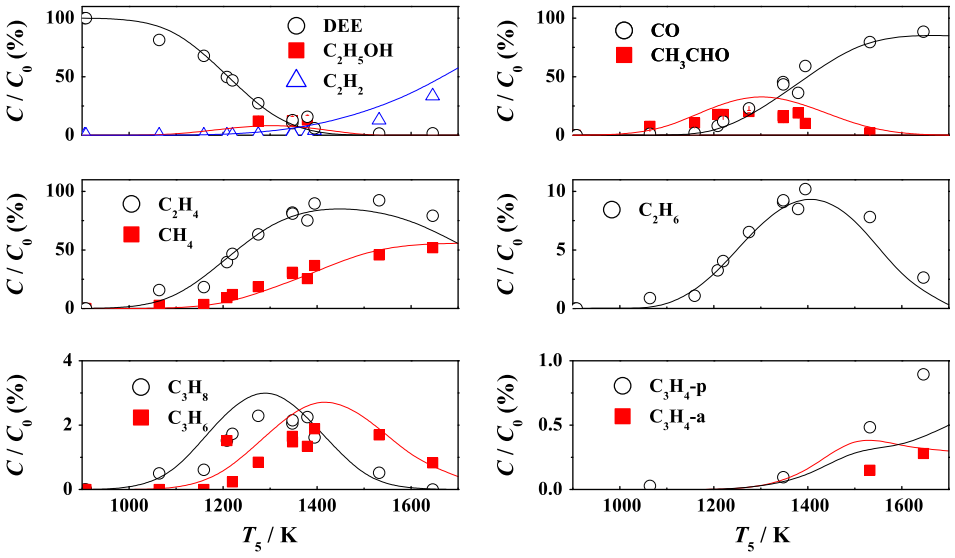

Fig. 3. Species profiles from the MHST for 2.0% DEE diluted in Ar at 1.0–2.9 atm, lines simulation and symbols experiment. C_0 and C denote initial concentration of DEE and concentration of chemical species after shock heat. Effective heating times used at 900 K, 1000 K, 1100 K, 1200 K, 1300 K, 1400 K, 1500 K, 1600 K and 1700 K were 1800, 1730, 1650, 1580, 1500, 1430, 1350 and 1200 μs, respectively.

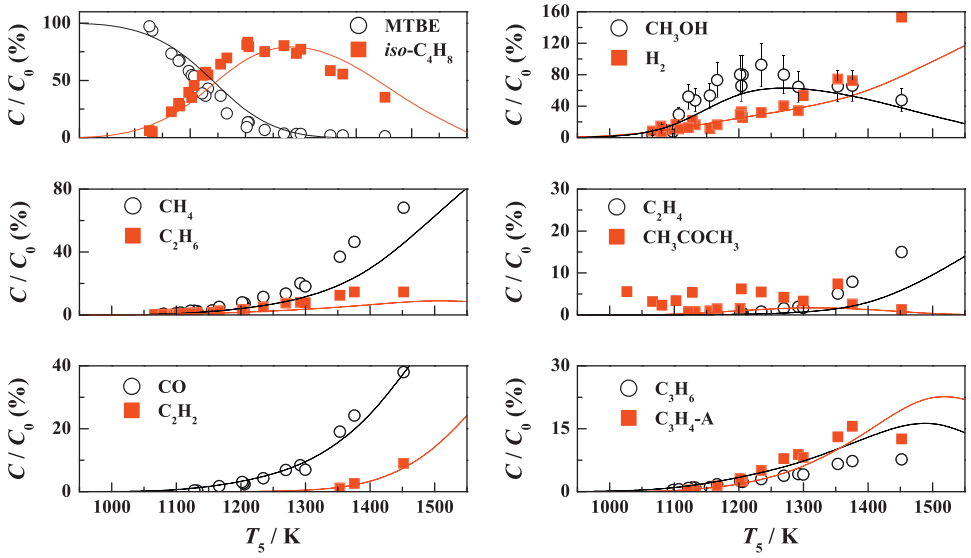

Fig. 4. Species profiles from the MHST for 1.0% MTBE diluted in Ar at 1.0–2.7 atm, lines simulation and symbols experiment. C_0 and C denote initial concentration of MTBE and concentration of chemical species after shock heat. Effective heating times used at 900 K, 1000 K, 1100 K, 1200 K, 1300 K, 1400 K, 1500 K and 1600 K were 2300, 2210, 2100, 1990, 1870, 1760, 1650 and 1500 μs, respectively.

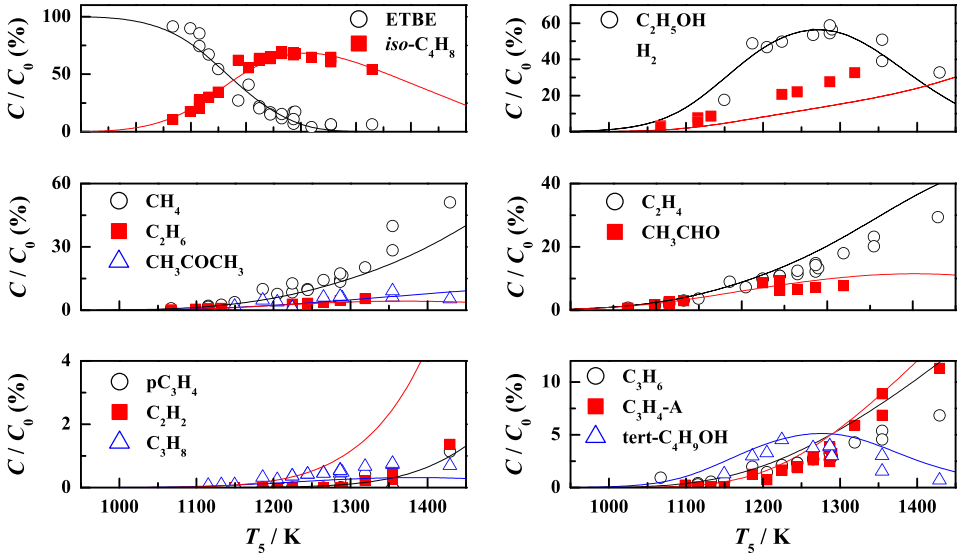

Fig. 5. Species profiles from the MHST for 3.0% ETBE diluted in Ar at 1.0–2.7 atm, lines simulation and symbols experiment. C_0 and C denote initial concentration of ETBE and concentration of chemical species after shock heat. Effective heating times used at 900 K, 1000 K, 1100 K, 1200 K, 1300 K, 1400 K and 1500 K were 1410, 1360, 1310, 1270, 1230, 1180 and 1130 μs, respectively.

calculated barrier heights for reactions (755), (670), (805), (783) and (804) were 65.2 kcal mol^{-1}, 65.2 kcal mol^{-1}, 63.4 kcal mol^{-1}, 60.8 kcal mol^{-1} and 60.6 kcal mol^{-1}, respectively. The difference in energies between 65.2 kcal mol^{-1} and 60.6 kcal mol^{-1} results in a variation of 5.5 times in reaction rate at 1300 K, so that MTBE [36] and ETBE mainly decompose via uni-molecular elimination reactions forming iso-butene and an alcohol.

The induction times of ȮH radical production measured by a standard-type shock tube (STST) for the mixtures 0.1% MTBE, 1.0% H_2, 1.0% O_2 in Ar and 0.1% ETBE, 1.0% H_2, 1.0% O_2 in Ar were newly obtained with the same method used in EME [4] and DEE [1]. A typical pressure and OH absorbance profiles are shown in Fig. 6. The results of induction times are shown together with that of iso-butene [37] in Fig. 7. As described above MTBE and ETBE preferentially decompose via uni-molecular elimination reactions to form methanol or ethanol and iso-butene. It implies that iso-butene chemistry influences the reactivity of MTBE and ETBE oxidation at high temperatures. The induction times of MTBE and ETBE mixtures is very similar to iso-butene mixture, while EME and DEE mixtures show shorter induction times compared to MTBE, ETBE and iso-butene. Iso-butene reacts with reactive atoms and radicals to produce 2-methylallyl radical, which subsequently decomposes to methyl radical and allene. Iso-butene converts reactive radicals to relatively unreactive methyl radicals. Therefore, iso-butene produced from MTBE and ETBE decompositions via uni-molecular reactions inhibits its reactivity of combustion systems [37].

5. Conclusions

As described above MTBE and ETBE preferentially decompose via uni-molecular elimination reactions to form methanol or

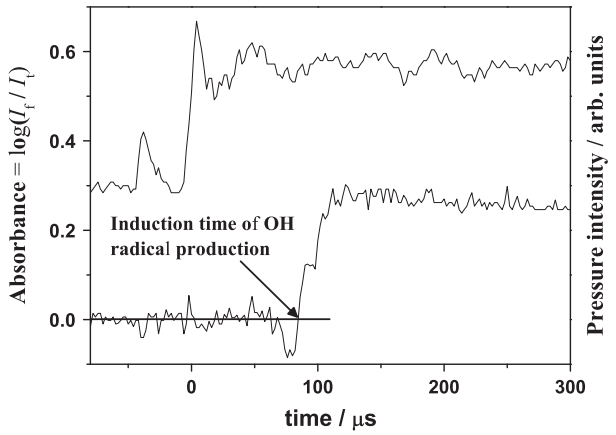

Fig. 6. Typical pressure and absorbance profiles at 306.7 nm from the STST for 0.1% ETBE, 1.0% H_2 and 1.0% O_2 diluted in Ar. OH radical absorbs light at this wavelength. T_5 = 1674 K, P_5 = 2.3 atm. I_f and I_t correspond to the incident and transmitted light intensity.

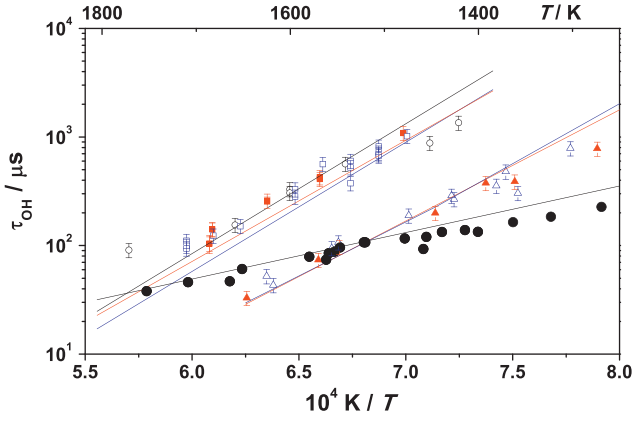

Fig. 7. Temperature dependence of τ_{OH} from the STST at P_5 = 1.4–2.6 atm (P_1 = 50 Torr), lines simulation symbols experiment; ○, 0.1% *iso*-C_4H_8 [37], 1% H_2, 1% O_2 in Ar; ■, 0.1% MTBE (this work), 1% H_2, 1% O_2 in Ar; □, 0.1% ETBE (this work), 1% H_2, 1% O_2 in Ar; △, 0.1% EME [4], 1% H_2, 1% O_2 in Ar; ▲, 0.1% DEE [1], 1% H_2, 1% O_2 in Ar; •, 1% H_2, 1% O_2 in Ar.

ethanol and iso-butene. Consequently, iso-butene chemistry greatly influences the reactivity of MTBE and ETBE oxidation at high temperatures. The induction times of MTBE and ETBE mixtures are very similar to iso-butene mixtures, while EME and DEE mixtures show shorter induction times relative to MTBE, ETBE and iso-butene. Iso-butene produced from MTBE and ETBE decompositions via uni-molecular reactions inhibits reactivity of the combustion system. Thus, uni-molecular elimination reactions of ethers play an important role in the pyrolysis and oxidation at high temperature.

Appendix A. Supplementary data

Supplementary data associated with this article can be found, in the online version, at doi:10.1016/j.combustflame.2010.10.012.

References

[1] K. Yasunaga, F. Gillespie, J.M. Simmie, H.J. Curran, Y. Kuraguchi, H. Hoshikawa, M. Yamane, Y. Hidaka, J. Phys. Chem. A 34 (2010) 9098–9109.
[2] M. Yahyaoui, N. Djebaili-Chaumeix, P. Dagaut, C.-E. Paillard, Energy Fuels 22 (2008) 3701–3708.
[3] T. Ogura, Y. Sakai, A. Miyoshi, M. Koshi, P. Dagaut, Energy Fuels 21 (2007) 3233–3239.
[4] K. Yasunaga, T. Koike, H. Hoshikawa, Y. Hidaka, Proc. Combust. Inst. 31 (2007) 313–320.
[5] K. Yasunaga, Y. Hidaka, A. Akitomo, T. Koike, Shock Waves 1 (2009) 165–169.
[6] K. Yasunaga, Y. Kuraguchi, Y. Hidaka, O. Takahashi, H. Yamada, T. Koike, Chem. Phys. Lett. 451 (2008) 192–197.
[7] C. Morley, Gaseq v0.79, <http://www.arcl02.dsl.pipex.com/gseqrite.htm>.
[8] Y. Hidaka, S. Shiba, H. Takuma, M. Suga, Int. J. Chem. Kinet. 17 (1985) 441–453.
[9] Y. Hidaka, T. Nakamura, A. Miyauchi, T. Shiraishi, H. Kawano, Int. J. Chem. Kinet. 21 (1989) 643–666.
[10] Y. Hidaka, K. Hattori, T. Okuno, K. Inami, T. Abe, T. Koike, Combust. Flame 107 (1996) 401–417.
[11] Y. Hidaka, K. Kimura, K. Hattori, T. Okuno, Combust. Flame 106 (1996) 155–167.
[12] Y. Hidaka, T. Higashihara, T. Nishimori, K. Sato, Y. Henmi, R. Okuda, K. Inami, Combust. Flame 117 (1999) 755–776.
[13] E.R. Ritter, J.W. Bozzelli, Int. J. Chem. Kinet. 23 (1991) 767–778.
[14] S.W. Benson, Thermochemical Kinetics, John Wiley & Sons, New York, 1976.
[15] S.E. Stein, R.L. Brown, in: P.J. Linstrom, W.G. Mallards, (Eds.), Structure and Properties Group Additivity Model in NIST Chemistry Webbook, NIST Standard Reference Database Number 69, National Institute of Standards and Technology, Gaithersburg MD, 2005, pp. 20899 <http://webbook.nist.gov>.
[16] S.L. Fisher, F.L. Dryer, H.J. Curran, Int. J. Chem. Kinet. 32 (2000) 713–740.
[17] W. Tsang, J. Phys. Chem. Ref. Data 17 (1988) 887–952.
[18] W. Tsang, J. Phys. Chem. Ref. Data 19 (1990) 1–68.
[19] Frisch M.J. et al., Gaussian 03, Revision D.01, Gaussian, Inc., Wallingford, CT, USA, 2004.
[20] A.M. Dean, J. Phys. Chem. 89 (1985) 4600–4608.
[21] A.M. Dean, J.M. Bozzelli, E.R. Ritter, Combust. Sci. Technol. 80 (1991) 63–85.
[22] R.G. Gilbert, K. Luther, J. Troe, Ber Bunsenges. Phys. Chem. 87 (1983) 169–177.
[23] T. Ogura, A. Miyoshi, M. Koshi, Phys. Chem. Chem. Phys. 9 (2007) 5133–5142.
[24] C. Zhou, J.M. Simmie, H.J. Curran, Phys. Chem. Chem. Phys. 12 (2010) 7221–7233.
[25] J.P. Orme, H.J. Curran, J.M. Simmie, J. Phys. Chem. A 110 (2006) 114–131.
[26] E.L. Petersen, D.M. Kalitan, S. Simmons, G. Bourque, H.J. Curran, J.M. Simmie, Proc. Combust. Inst. 31 (2007) 447–454.
[27] S. Gallagher, H.J. Curran, W.K. Metcalfe, D. Healy, J.M. Simmie, G. Bourque, Combust. Flame 153 (2007) 316–333.
[28] D. Healy, H.J. Curran, S. Dooley, J.M. Simmie, D.M. Kalitan, E.L. Petersen, G. Bourque, Combust. Flame 155 (2008) 451–461.
[29] D. Healy, H.J. Curran, J.M. Simmie, D.M. Kalitan, C.M. Zinner, A.B. Barrett, E.L. Petersen, G. Bourque, Combust. Flame 155 (2008) 441–448.
[30] D. Healy, M.M. Kopp, N.L. Polley, E.L. Petersen, G. Bourque, H.J. Curran, Energy Fuels 24 (3) (2010) 1617–1627.
[31] D. Healy, D.M. Kalitan, C.J. Aul, E.L. Petersen, G. Bourque, H.J. Curran, Energy Fuels 24 (3) (2010) 1521–1528.
[32] D. Healy, N.S. Donato, C.J. Aul, E.L. Petersen, C.M. Zinner, G. Bourque, H.J. Curran, Combust. Flame 157 (2010) 1526–1539.
[33] D. Healy, N.S. Donato, C.J. Aul, E.L. Petersen, C.M. Zinner, G. Bourque, H.J. Curran, Combust. Flame 157 (2010) 1540–1551.
[34] N. Donato, C. Aul, E. Petersen, C. Zinner, H. Curran, G. Bourque, J. Eng. Gas Turb. Power 132 (5) (2010). Paper Number: 051502 (9 pages).
[35] Chemkin-Pro™, Reaction Design Inc., San Diego, Calif.
[36] M.P. Dunphy, J.M. Simmie, Combust. Flame 85 (1991) 489–498.
[37] K. Yasunaga, Y. Kuraguchi, R. Ikeuchi, H. Masaoka, O. Takahashi, T. Koike, Y. Hidaka, Proc. Combust. Inst. 32 (2009) 453–460.